International Conference on Textile Composites and Inflatable Structures
STRUCTURAL MEMBRANES 2011
E. Oñate, B. Kröplin and K.-U.Bletzinger (Eds)

MECHANICS OF LOCAL BUCKLING IN WRAPPING FOLD MEMBRANE

YASUTAKA SATOU* AND HIROSHI FURUYA*

*Department of Built Environment
Tokyo Institute of Technology
4259-G3-6 Nagatsuta, Midori-ku, Yokohama 226-8502, Japan
e-mail: satou@space.enveng.titech.ac.jp

Key words: Buckling, Wrapping Fold, Solar Sail, Membrane Structure

Abstract. Mechanics of a local buckling, which is induced by wrapping fold of a creased membrane, is discussed experimentally, theoretically, and numerically in this paper to examine the condition for the local buckling. The theoretical analysis is performed by introducing one-dimensional wrapping fold model, and the dominant parameters of the condition for the local buckling are obtained, which are expressed by the tensile force, the membrane thickness, and the radius of the center hub. The experimental results indicate that the interval of the local buckling is proportional to the diameter of the center hub, and the results are qualitatively agreement with the FEM results.

1 INTRODUCTION

There is currently much interested in the use of large deployable space membranes for several lightweight space structures; solar sails[1], large aperture antennas, sunshields, solar power satellites, and et al. As the space membranes are folded and packed in a rocket and deployed in the space, the fold properties affect the deployment dynamics, and hence, the fold is one of the significant technical issues to realize the space membranes. For example, the membrane is desired to be folded simply with compact storage. Also, in the folding process, the damages to the membrane have to be avoided.

One of the folds for the space membrane is wrapping fold[2]. In the course of the wrapping fold of a creased membrane, local buckling is observed repeatedly as shown in Fig.1. This local buckling is induced by the compressive stress in the inner membrane. When the local buckling occurs, the layer thickness of the wrapped membrane is locally increased, and hence, the package volume is increased. Also, when the compressive stress is concentrated by the local buckling, the membrane would be damaged. Thus, it is significant to investigate the mechanics of the local buckling.

In this paper, the mechanics of the local buckling in a wrapping fold membrane is examined experimentally, theoretically, and numerically to determine the condition for the local buckling and the interval of the local buckling. We focus on the wrapping fold around a cylindrical center hub, which is used in IKAROS[1]. At first, the wrapping fold experiments for a creased membrane are performed to indicate the local buckling behavior in terms of the tensile force for wrapping, the diameter of the center hub, and the membrane thickness, where the local buckling is treated with the interval of that. Next, to determine the dominant parameters of the condition for the local buckling, theoretical analysis is performed by introducing a one-dimensional model. Then, the experimental and theoretical results are evaluated by FEM analyses. Finally, the condition for the local buckling and the interval are discussed.

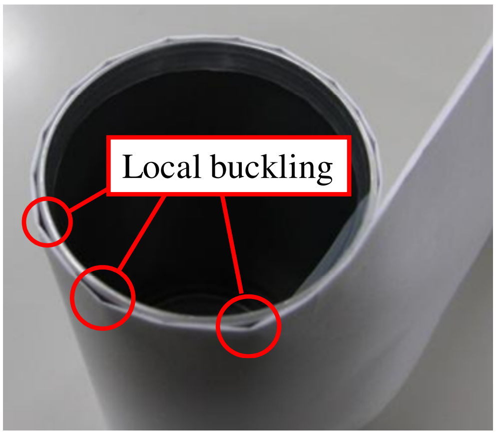

Figure 1: Overview of local buckling

2 WRAPPING FOLD EXPERIMENTS

Figure 2 indicates the cross-section of the wrapping fold membrane. We assume that the cross-section of the wrapping fold is the repeating structure, and hence, the selected area in Fig.2 is modeled for the membrane specimen of the wrapping fold experiments. To evaluate the crease quantitatively, we introduce a layer pitch h, which indicates the thickness per a membrane of the folded thickness.

Figure 3 indicates the experimental setup. As shown in the front view in Fig.3a, the upper end of the membrane specimen is attached to the center hub by Kapton tape. To apply the tensile force to the membrane, the lower end of the membrane specimen is sandwiched by steel brackets, and weights are applied to the steel brackets as shown in Fig.3a,b. On the both sides of the membrane in Fig.3a, the creases are generated, which are cl and cr. These creases cl and cr correspond to the creases indicated in the cross-sectional view, Fig.3c.

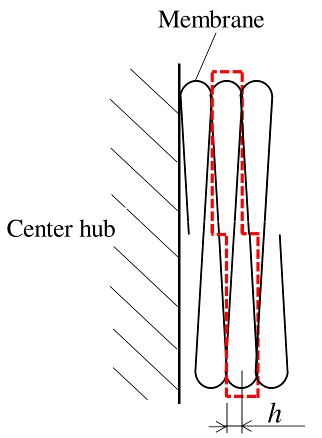

Figure 2: Cross-section of experimental model

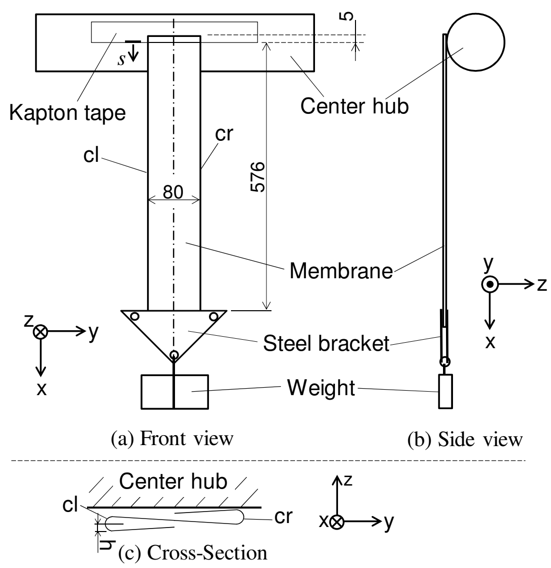

Figure 3: Experimental setup

3 ONE-DIMENSIONAL THEORETICAL ANALYSIS

A one-dimensional model for a wrapping fold membrane is introduced, and the theoretical analysis for the model is formulated to examine the mechanics of the local buckling.

3.1 One-dimensional wrapping model

Figure 4a indicates a one-dimensional analytical model of a wrapping fold membrane. In the figure, r and T represent the radius of the cylindrical center hub and the tensile force, respectively. In the model, we treat the wrapped membrane as a one-dimensional model to simplify the mechanics of the wrapping fold. To this end, the cross-section has to be assumed. Fig.5a indicates the cross-section of the wrapping fold membrane of the membrane specimen for the experiments, where t, s, and l_0 represent the membrane thickness, the body fixed system of the membrane, and the overall length of the membrane along the body fixed system. As shown in the figure, the layer pitch around the crease is thicker than that of the other area, we introduce a cylindrical cross-sectional model as shown in Fig.5b, where the radius and the thickness are a and t'. In that case, we have to consider the equivalent in-plane stiffness as,

$$Etl_0 = Et'2\pi a \tag{1}$$

where, E is the Young's modulus.

For the one-dimensional model shown in Fig.4a, we assume that the local buckling occurs in $\cdot\cdot\, b_{n-2}$ and b_{n-1}. As the layer pitch becomes small in the position of the local buckling as shown in Fig.1, the bending moment is small at b_{n-1}, and thus, the bending moment becomes maximum somewhere between b_{n-1} and A. We define that position as b_n, where the local buckling is about to occur, and l_b corresponds to the interval of the local buckling.

To examine the condition for the local buckling at b_n, we focus on the membrane element between b_{n-1} and b_n as shown in Fig.4b. We assume that the membrane element contacts with the center hub from $\theta = 0$ to θ_c, and the contact area is l_c, where $\theta = 0$ at b_n, and the membrane dose not contact with the center hub in the area δ. The equilibriums of the force in the membrane element in the z-direction and in the x-direction are,

$$T + R_{n-1}sin\theta - Tcos\theta - \int_0^{\theta_c} qsin\theta rd\theta = 0 \tag{2}$$

$$R_n + R_{n-1}cos\theta + Tsin\theta - \int_0^{\theta_c} qcos\theta rd\theta = 0 \tag{3}$$

Also, the equilibrium of the moment in the membrane element is,

$$(R_{n-1}cos\theta + Tsin\theta)rsin\theta - \int_0^{\theta_c} qcos\theta rsin\theta rd\theta - M_n + M_{n-1} = 0 \tag{4}$$

where, q, R_n, R_{n-1}, M_n, and M_{n-1} represent the distributed contact force applied by the center hub, the reaction force at b_n, the reaction force at b_{n-1}, the moment at b_n, and the moment at b_{n-1}, respectively. The distributed contact force q is derived by the equation for a wrapped belt[3] as,

$$q = T/r \tag{5}$$

where, the one-dimensional wrapping by the tensile force T around the cylindrical center hub of r radius are assumed. As the layer pitch is small at b_{n-1}, we assume the layer pitch at b_{n-1} becomes $2t'$. In that case, the moment at b_{n-1} is derived as,

$$M_{n-1} = \frac{EI_{n-1}}{r} \cong \frac{E\pi at'^3}{12r} \tag{6}$$

where I_{n-1} is the moment of inertia of area at b_{n-1}. By solving the simultaneous equations Eq.(2)-(4), and using Eq.(5) and (6), the moment at b_n is derived as,

$$M_n = \frac{E\pi at'^3}{12r} + Tr\{1 - cos(\frac{l_b}{r})cos(\frac{l_c}{r}) - \frac{1}{2}sin^2(\frac{l_c}{r})\} \tag{7}$$

As the contact area between the membrane and the center hub cannot be derived by the one-dimensional model, the effect of δ in Fig.4b on the moment Eq.(7) is examined. We define F as,

$$F = 1 - cos(\frac{l_b}{r})cos(\frac{l_c}{r}) - \frac{1}{2}sin^2(\frac{l_c}{r}) \tag{8}$$

and, Eq.(8) is expressed with δ as,

$$F = 1 - cos(\tfrac{l_b}{r})cos(\tfrac{l_b-\delta}{r}) - \tfrac{1}{2}sin^2(\tfrac{l_b-\delta}{r}) \tag{9}$$
$$=1 - cos^2(\frac{l_b}{r})cos(\frac{\delta}{r}) - sin(\frac{l_b}{r})cos(\frac{l_b}{r})sin(\frac{\delta}{r})$$
$$\frac{1}{2}\{sin^2(\frac{l_b}{r})cos^2(\frac{\delta}{r}) - 2sin(\frac{l_b}{r})cos(\frac{\delta}{r})cos(\frac{l_b}{r})sin(\frac{\delta}{r}) + cos^2(\frac{l_b}{r})sin^2(\frac{\delta}{r})\}$$

When we assume δ is sufficiently smaller than r, the following equations are derived as,

$$sin(\frac{\delta}{r}) \cong 0, cos(\frac{\delta}{r}) \cong 1 \tag{10}$$

Using Eq.(10) and (10), F is expressed as,

$$F \cong 1 - cos^2(\frac{l_b}{r}) - \frac{1}{2}sin^2(\frac{l_b}{r}) \tag{11}$$

Thus, in this paper, we treat l_c as l_b.

Next, we discuss the condition for the local buckling. The stress in the inner membrane at b_n is expressed as,

$$\sigma_{bn} = -\frac{M_n}{I_n}a + \frac{T}{2\pi a t'} \tag{12}$$

where I_n is the moment of inertia of area at b_n, and expressed as,

$$I_n = \frac{\pi\{a^4 - (a-t')^4\}}{4} \tag{13}$$

The 2nd term on the right hand side of Eq.(12) is the tensile stress by the tensile force, T. As the local buckling occurs when σ_{bn} is smaller than the buckling stress σ_{cr}, the condition for the local buckling is,

$$-\frac{M_n}{I_n}h + \frac{T}{2\pi a t'} < -\sigma_{cr} \tag{14}$$

As the cross-section has the curvature $1/a$, the compressive buckling stress of the cylinder is applied to the buckling stress σ_{cr} as,

$$\sigma_{cr} = \frac{1}{\sqrt{3(1-\nu^2)}}\frac{Et'}{a} \tag{15}$$

where, ν is Poisson's ratio.

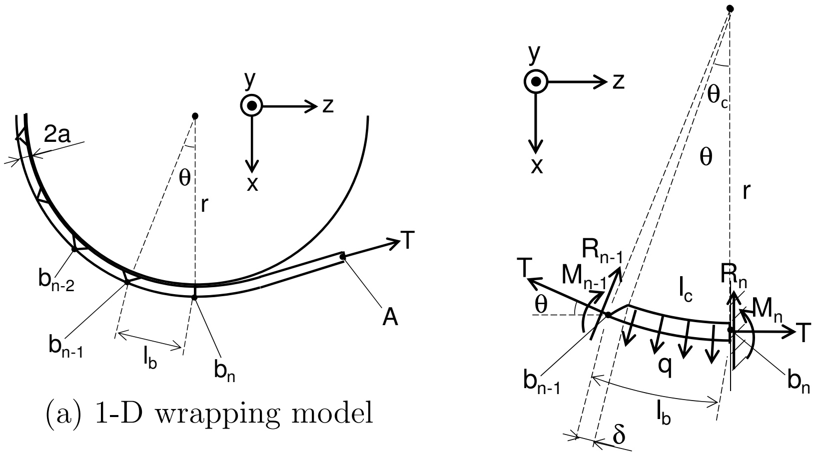

(a) 1-D wrapping model

(b) Membrane element

Figure 4: One-dimensional analytical model of wrapping fold membrane

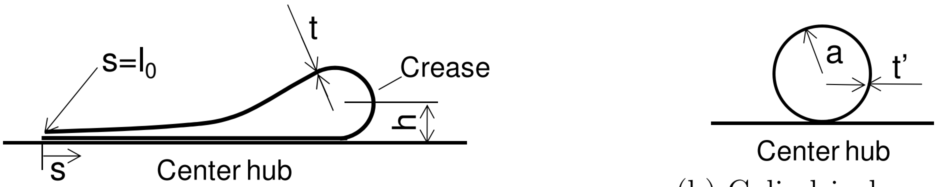

(a) Wrapping fold membrane

(b) Cylindrical model

Figure 5: Cross-sectional model

3.2 Dominant parameters for local buckling

The dominant parameters for the local buckling are examined using Eq.(14). By using Eq.(7) and (8), Eq.(14) is expressed as,

$$-\frac{a}{I_n}(M_{n-1} + TrF) + \frac{T}{2\pi a t'} < -\sigma_{cr} \tag{16}$$

As the layer pitch is small in the position of the local buckling, which is indicated in Fig.1, the bending moment M_{n-1} is sufficiently smaller than the 2nd term in the parentheses on the left hand side of Eq.(16), TrF. The value of a and I_n is determined by T, r, and t in the wrapping fold process. When the radius of the center hub is sufficiently larger than the interval of the local buckling, l_b is sufficiently smaller than r, and hence, F in the Eq.(16) becomes roughly constant. Based on the above discussion, the condition for the local buckling is mainly affected by T, r, and t' in Eq.(16). Considering the form of Eq.(16) and (1), the dominant parameters of the condition for the local buckling are T/t

and Tr. Using these dominant parameters, Eq.(16) is expressed as,

$$(Tr) > \frac{1}{F}\{\frac{I_n}{a}(\frac{1}{l_0}\frac{T}{t} + \sigma_{cr}) - M_{n-1}\} \tag{17}$$

4 FEM ANALYSIS

FEM analyses are performed for the wrapping fold membrane to evaluate the experiments and the theoretical analysis. The FEM analyses are demonstrated with ABAQUS[4], a commercial software. As the wrapping fold process induces geometrical nonlinearity, the analysis procedure is geometrical nonlinear and static, where the implicit integration scheme is employed. The analysis procedure is carried out by applying General Static and NLgeom option. To stabilize the FEM analyses numerically, the numerical wrapping fold process is significant. We introduce a numerical creasing process proposed in our previous research[5].

5 RESULTS AND DISCUSSION

In this section, we discuss the results obtained by the experiments, by the theoretical analysis, and by the FEM analyses to examine the condition for the local buckling and the interval of the local buckling. In the theoretical analysis and the FEM analyses, Young's modulus and Poisson's ratio are set to be $4.8GPa$ and 0.30, respectively.

5.1 Condition for local buckling

Figure 6 indicates the condition for the local buckling. The symbol ◯ and × indicate the experimental data where the local buckling occurs and doesn't occur, respectively. The experimental data are plotted for the dominant parameters obtained by the theoretical analysis. The solid and the broken lines show the condition for the local buckling calculated by Eq.(17). As the distribution of the experimental data can be divided into two regions, the effectiveness of the dominant parameters are confirmed. When we apply a proper value to a, the condition for the local buckling obtained by the experiments can be qualitatively expressed by the one-dimensional wrapping fold model. On the other hand, to clarify the condition quantitatively, the cross-sectional configuration of the wrapping fold membrane has to be improved.

5.2 Interval of local buckling

As the interval of the local buckling is affected by the experimental condition, the interval is selected as the parameter to examine the mechanics of the local buckling. In this section, we focus on the effects of the tensile force and the diameter of the center hub on the interval.

The effects of the tensile force on the interval of the local buckling obtained by the experiments are indicated in Fig.7. The membrane thickness and the diameter of the center hub are $50\mu m$ and $30mm$, respectively. For these data, the solid line and the

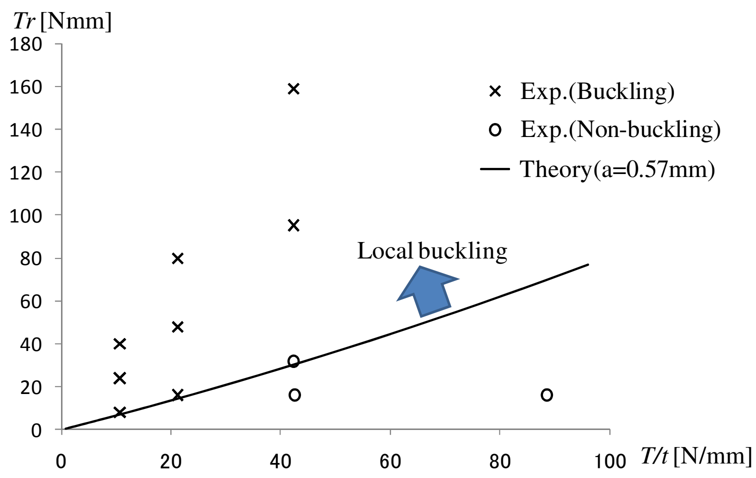

Figure 6: Condition for local buckling

broken line represent the results of the crease *cl* and that of *cr*, where these results are the average values of the intervals in each round; 1st, 2nd, and 3rd round. When the tensile force is increased from $0.013N/mm$ to $0.027N/mm$, the interval is decreased up to 62% (*cr*, 3rd). On the other hand, when the tensile force is increased from $0.027N/mm$ to $0.053N/mm$, the interval is decreased up to 81% (*cr*, 3rd). Thus, although the interval is decreased as the tensile force becomes larger, the rate of the decrement is also reduced. These results are qualitatively expressed by the theoretical analysis.

To examine the effects of the diameter of the center hub on the interval of the local buckling, three kinds of diameters for the center hub are used; $30, 90, and 150mm$. The experimental, theoretical, and FEM results are indicated in Fig.8. The tensile force and the membrane thickness are $0.027N/mm$ and $50\mu m$, respectively. The black dots and the white dots represents the experimental and the FEM results, where the solid line and the broken line are the results of the crease *cl* and that of *cr*, respectively. Also, these data are the average value of the intervals in the 1st round. When the diameter of the center hub is increased from $30mm$ to $90mm$, the interval is increased up to 2.8 times (*cl*), for the experimental data. Also, when the diameter is increased from $90mm$ to $150mm$, the interval is increased up to 1.6 times (*cr*). These results indicate that the interval is almost proportional to the diameter of the center hub. These experimental results are qualitatively expressed by the FEM results. However, too large interval is obtained by the theoretical analysis. It seems that this result is due to the constant value of a, because in the experiments, the layer pitch becomes large as the diameter of the center hub is increased.

6 CONCLUSIONS

Mechanics of the local buckling was examined to determine the condition for the local buckling. To treat the mechanics, the interval of the local buckling was introduced.

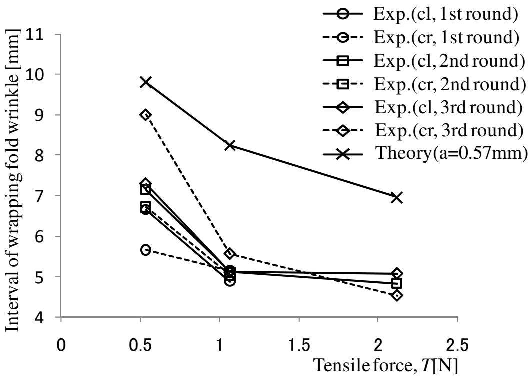

Figure 7: Effects of tensile force

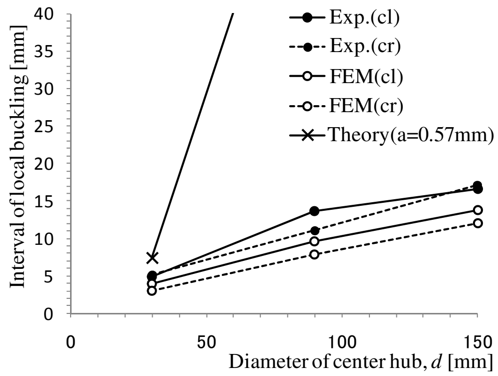

Figure 8: Effects of diameter of center hub

The experimental data indicated that the interval became smaller as the tensile force was increased, and was almost proportional to the diameter of the center hub. In the theoretical analysis, a one-dimensional wrapping model was introduced to examine the mechanics of the local buckling. The dominant parameters for the condition for the local buckling, which were expressed by the tensile force, the membrane thickness, and the radius of the center hub. Also, the experimental data were qualitatively expressed by the one-dimensional wrapping model.

REFERENCES

[1] Furuya, H. Mori, O. Sawada, H. Okuizumi, N. Shirasawa, Y. Natori, M. C. Miyazaki, Y. and Matsunaga, S. Manufacturing and Folding of Solar Sail "IKAROS". AIAA 2011-1967. CD-ROM Proc. *52th AIAA/ASME/ASCE/AHS/ASC Structures, Structural Dynamics and Materials Conference*. (2011) :1–4.

[2] Guest, S.D. and Pellegrino, S. Inextensional Wrapping of Flat Membranes. *First International Conference on Structural Morphology*. (1992) :203–215.

[3] Timoshenko, S. and Young, D. H. *Engineering Mechanics*. McGraw-Hill, (1956).

[4] ABAQUS user's manual, Ver. 6.8, ABAQUS Inc., (2008).

[5] Satou, Y. and Furuya, H. Mechanical Properties of Wrapping Fold Wrinkles in Large Space Membrane. 2011-c-32, CD-ROM Proc., *28th International Symposium on Space Technology and Science*. (2011) :1–6.